J Mater Sci (2009) 44:855–860
DOI 10.1007/s10853-008-3128-6

Low-temperature sintering of ZrW_2O_8–SiO_2 by spark plasma sintering

Kenji Kanamori · Tohru Kineri · Ryohei Fukuda · Takafumi Kawano · Keishi Nishio

Received: 2 September 2008 / Accepted: 20 November 2008 / Published online: 11 December 2008

Abstract Amorphous ZrW_2O_8 powder and amorphous SiO_2 powder were prepared by a sol–gel process as raw materials, and high-density ZrW_2O_8–SiO_2 were successfully prepared at a much lower temperature of 923 K for a much shorter holding time of 10 min by spark plasma sintering (SPS) method rather than by conventional melt-quenching method. The relative densities of $0.85ZrW_2O_8$–$0.15SiO_2$ and $0.70ZrW_2O_8$–$0.30SiO_2$ were 99.4% and 96.6%, respectively. The combined technique of a sol–gel process and SPS should enable us to prepare the varied types of high-density composites of ZrW_2O_8 without severe thermal cracking caused by melt-quenching. The thermal expansion properties and dielectric properties of ZrW_2O_8–SiO_2 were also investigated.

K. Kanamori (✉)
Graduate School of Science and Engineering, Tokyo University of Science, Yamaguchi, Sanyo-Onoda-shi,
Yamaguchi 756-0884, Japan
e-mail: je107607@ed.yama.tus.ac.jp

T. Kineri
Department of Materials Science and Environmental Engineering, Tokyo University of Science, Yamaguchi,
Sanyo-Onoda-shi, Yamaguchi 756-0884, Japan

R. Fukuda
Enhanced Ceramics Substrate Department, Sumitomo Metal (SMI) Electronics Devices Inc., Mine-shi,
Yamaguchi 759-2212, Japan

T. Kawano
Inorganic Specialty Products Research Laboratory,
Ube Industries, Ltd., Ube-shi, Yamaguchi 755-8633, Japan

K. Nishio
Department of Materials Science and Technology, Tokyo University of Science, Noda-shi, Chiba 278-8510, Japan

Introduction

ZrW_2O_8 exhibits isotropic negative thermal expansion in a wide temperature range, 0.3–1050 K, so it can be used as a compensator material for controlling the thermal expansion coefficient (CTE) of ceramics, metals, and polymers [1–4].

From the ZrO_2–WO_3 pseudo binary phase diagram, the thermodynamically stable region of ZrW_2O_8 is only limited to between 1378 and 1530 K, and ZrW_2O_8 is kinetically stable at temperatures lower than its thermal decomposition temperature of 1050 K [5]. Therefore, ZrW_2O_8 must be rapidly quenched in that high-temperature region to preserve it at room temperature [6–8]. However, the melt-quenching method has several problems such as the changes of chemical composition due to the volatilization of WO_3 at the high-temperature region and the crack generation in ZrW_2O_8 due to the rapid quenching.

Recently, low-temperature preparation processes for ZrW_2O_8 have been studied. Xing et al. have reported preparation by a hydrothermal process [9, 10]. Sleight et al. have reported preparation by an aqueous sol–gel process, using $ZrOCl_2 \cdot 8H_2O$ and $(NH_4)_6H_2W_{12}O_{40}$ as raw materials [11, 12]. The single-phase ZrW_2O_8 is prepared by the sol–gel process at 873 K for 10 h, whereas it is very difficult to prepare the high-density ZrW_2O_8. Wilkinson et al. have reported preparation by a non-hydrolytic sol–gel process [13]. The ZrW_2O_8 gel is amorphous below 873 K and crystallizes into trigonal ZrW_2O_8 at about 1013 K. However, in all the preparation processes of ZrW_2O_8, the conventional melt-quenching method was essential for preparing the high-density ZrW_2O_8.

Spark plasma sintering (SPS) method is similar to conventional hot-pressing method in that the precursor is loaded in a graphite die, and a uniaxial pressure is applied during the sintering process. However, instead of using an external heating source, a pulsed direct current is allowed to pass through the electrically conducting die and, in appropriate cases, also through the sample [14]. The SPS enables metals and ceramics powder compacts to be sintered at relatively lower temperatures and in much shorter sintering periods compared with conventional hot-pressing method [15–19].

SiO_2 has attracted considerable attention because its dielectric constant is extremely low (≈ 4) [20]. The low dielectric constant reduces the delay time of electronic signal transmission, that is, microwave telecommunication can transmit a large amount of information at a very high speed.

There are many reports on the composites of ZrW_2O_8, such as ZrW_2O_8–ZrO_2 [21–25], ZrW_2O_8–Cu [26, 27], and ZrW_2O_8-phenolic resin [28]. However, in all the preparation processes of the composites, the conventional melt-quenching method was also essential for preparing the high-density composites of ZrW_2O_8.

In this study, amorphous ZrW_2O_8 powder and amorphous SiO_2 powder were prepared by a sol–gel process as raw materials, and high-density ZrW_2O_8–SiO_2 were successfully prepared at a much lower temperature of 923 K for a much shorter holding time of 10 min by SPS rather than by conventional melt-quenching method. The combined technique of a sol–gel process and SPS should enable us to prepare the varied types of high-density composites of ZrW_2O_8 without severe thermal cracking caused by melt-quenching. The thermal expansion properties and dielectric properties of ZrW_2O_8–SiO_2 were also investigated.

Experimental procedure

Preparation of raw materials

Amorphous ZrW_2O_8 powder with a particle size of 50–300 nm was prepared by a sol–gel process, as described previously [29]. First, 0.0628 mol of WCl_6 (99%, Mitsuwa Chemicals Co., Ltd., Japan) was dissolved in ethyl alcohol at room temperature under a nitrogen gas atmosphere because tungsten alkoxides react with water and oxygen in air. Next, 0.0314 mol of $ZrOCl_2 \cdot 8H_2O$ (99%, Kishida Chemical Co., Ltd., Japan) was dissolved in a mixture of 100 mL of 2-butyl alcohol, 50 mL of ethyl alcohol, and 50 mL of distilled water. Then, the tungsten solution was poured into a zirconium solution to prepare the precursor sol, and this was stirred at room temperature for 72 h. The precursor sol was heated at between 351 and 358 K to prepare the precursor $ZrW_2O_7(OH)_2(H_2O)_2$. This precursor was calcined at 723 K for 12 h in air to prepare the amorphous ZrW_2O_8 powder.

Amorphous SiO_2 powder with a particle size of less than 63 μm was used in this study. First, 0.058 mol of $Si(OC_2H_5)_4$ (99%, Kishida Chemical Co., Ltd., Japan) was dissolved in 21 mL of ethyl alcohol at room temperature. Next, 11 mL of 0.18 mol/L HCl was added dropwise to the alkoxide solution of $Si(OC_2H_5)_4$ in order to accelerate the hydrolysis reactions of $Si(OC_2H_5)_4$, and the whole was heated at 315 K for 48 h in air to form silica gel. This gel was calcined at 1123 K for 3 h in air to prepare the amorphous SiO_2 powder. These powders for sintering were mixed in the volume fraction of $0.85ZrW_2O_8$–$0.15SiO_2$ and $0.70ZrW_2O_8$–$0.30SiO_2$.

Low-temperature sintering by SPS

About 3-g portions of ZrW_2O_8–SiO_2 powder were poured into the graphite dies having inner diameter of 20 mm and then pressed into pellets at 45 MPa. These pellets were sintered at 923 K for 10 min with a heating rate of about 60 K/min under a nitrogen gas atmosphere using the SPS apparatus (SPS-1050, Sumitomo Coal Mining Co., Ltd., Japan). The applied pressure of 45 MPa was held constant until the end of the sintering period. The sintering temperature of ZrW_2O_8–SiO_2 was measured with type-K thermocouples which were inserted into the wall of the graphite die. The prepared ZrW_2O_8–SiO_2 were re-oxidized in air at 873 K for 8 h.

Characterization

Each sample was identified with an X-ray diffractometer (UltimaIII, Rigaku, Japan). The IR spectra were recorded using KBr pellets on a Fourier transform infrared spectrometer (FT-IR: JIR-WINSPEC50, JEOL, Japan).

A microstructure analysis of each sample was performed with a field emission scanning electron microscope (FE-SEM: JSM-7000F, JEOL, Japan) equipped with an energy dispersive X-ray spectrometer (EDS: JED-2300, JEOL, Japan).

Each density of ZrW_2O_8–SiO_2 was measured by the Archimedes method, and each theoretical density of the composite ρ_{com} was calculated using the mixture rule:

$$\rho_{com} = V_1\rho_1 + V_2\rho_2, \quad (1)$$

where ρ_1, ρ_2, V_1, and V_2 are the density of ZrW_2O_8, the density of SiO_2, the volume fraction of ZrW_2O_8, and the volume fraction of SiO_2, respectively.

The thermal expansion properties of ZrW_2O_8–SiO_2 were measured with a thermal mechanical analyzer (TMA: TMA 4000S, Mac Science, Co., Ltd., Japan) at the heating and cooling rates of 5 K/min.

The dielectric properties of ZrW_2O_8–SiO_2 in a frequency range from 1 kHz to 1 MHz were measured with an impedance analyzer (4194A, Hewlett-Packard, USA) at 300 K. The Au electrodes were formed on the both surfaces of ZrW_2O_8–SiO_2. The microwave properties of ZrW_2O_8–SiO_2 were measured by a waveguide method with a network analyzer (8720ES, Agilent, USA) at a frequency of 8 GHz at 300 K.

Results and discussion

Phase identification of samples sintered by SPS

Figure 1 shows the X-ray diffraction patterns of ZrW_2O_8–SiO_2. The (a) and (b) patterns consisted of cubic ZrW_2O_8 and amorphous SiO_2. Figure 2 shows the FT-IR spectra of ZrW_2O_8–SiO_2. We assigned the main band centered at 1000, 910, and 875 cm^{-1} to WO_4 symmetric stretching vibration and those at 804, 764, and 742 cm^{-1} to WO_4 asymmetric stretching vibration [30]. The other band centered at ~ 1100 and ~ 470 cm^{-1} can be assigned to Si–O–Si asymmetric stretching vibration and Si–O–Si bending vibration, respectively [31]. As shown in Fig. 3, EDS analysis and backscattered scanning electron microscopy (BSE) revealed that the microstructures consisted of light gray grains (ZrW_2O_8) and dark black grains (SiO_2).

Thermal expansion properties of ZrW_2O_8–SiO_2

As shown in Fig. 4, thermal expansion hysteresis at a temperature range of 323–398 K was slightly observed in $0.70ZrW_2O_8$–$0.30SiO_2$, which indicates that physically bound water disturbs the torsion of WO_4 tetrahedra [32, 33]. On the contrary, thermal expansion hysteresis was not observed in $0.85ZrW_2O_8$–$0.15SiO_2$, which indicates that there are no micro cracks [34], and the density of $0.85ZrW_2O_8$–$0.15SiO_2$ is higher than that of $0.70ZrW_2O_8$–$0.30SiO_2$.

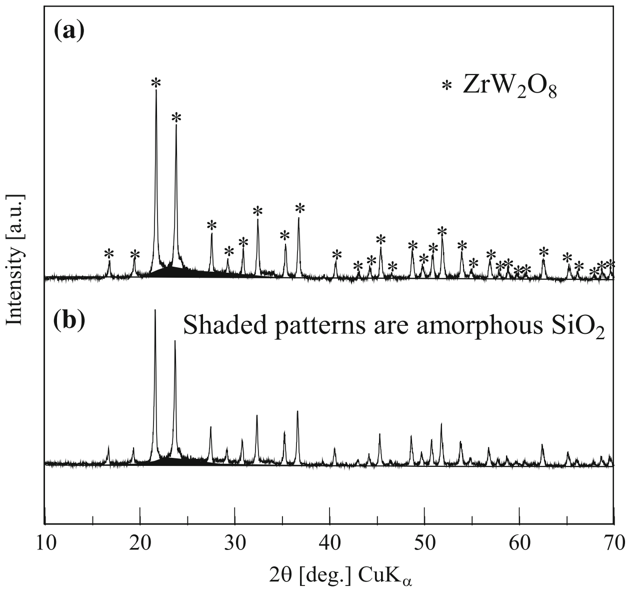

Fig. 1 X-ray diffraction patterns of (a) $0.70ZrW_2O_8$–$0.30SiO_2$ and (b) $0.85ZrW_2O_8$–$0.15SiO_2$

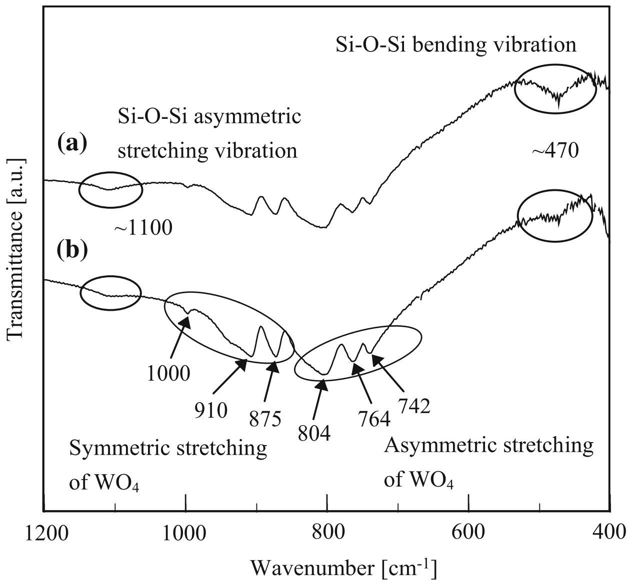

Fig. 2 FT-IR spectra of (a) $0.70ZrW_2O_8$–$0.30SiO_2$ and (b) $0.85ZrW_2O_8$–$0.15SiO_2$

The CTE of ZrW_2O_8–SiO_2 composites were considered by using the rule of mixtures (ROM) approximation [28]:

$$\alpha_{cal} = \alpha_1 V_1 + \alpha_2 V_2, \quad (2)$$

where α_1, α_2, V_1, and V_2 are the CTE of ZrW_2O_8 [35], the CTE of SiO_2 [20], the volume fraction of ZrW_2O_8, and the volume fraction of SiO_2, respectively. The experimental CTE of ZrW_2O_8–SiO_2 at a temperature range of 323–398 K represents "Data (A)" and that of ZrW_2O_8–SiO_2 at a temperature range of 473–673 K represents "Data (B)". The relative densities of $0.85ZrW_2O_8$–$0.15SiO_2$ and $0.70ZrW_2O_8$–$0.30SiO_2$ were 99.4% and 96.6%, respectively. As shown in Fig. 5, the both CTE of $0.85ZrW_2O_8$–$0.15SiO_2$ and $0.70ZrW_2O_8$–$0.30SiO_2$ well agreed with the ROM approximation (Eq. 2).

Dielectric properties of ZrW_2O_8–SiO_2

Figures 6 and 7 show the frequency dependence of the dielectric constant (ε_r) and dielectric loss ($\tan\delta$) of re-oxidized ZrW_2O_8–SiO_2, respectively. The $\tan\delta$ of reduced ZrW_2O_8–SiO_2 was too large to measure because SPS is usually performed in a reducing atmosphere in order to prevent the oxidation of graphite dies. To improve the problem, the reduced ZrW_2O_8–SiO_2 was re-oxidized at 873 K for 8 h in air. The ε_r and $\tan\delta$ of re-oxidized ZrW_2O_8–SiO_2 tended to decrease with increasing

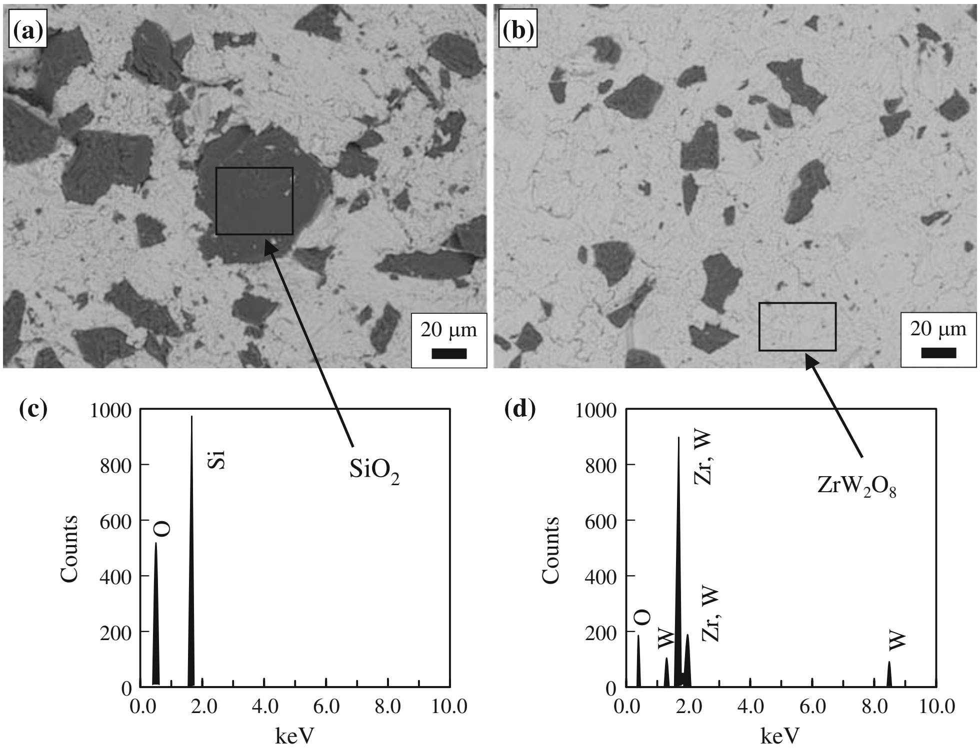

Fig. 3 BSE images of the polished surfaces of (**a**) $0.70ZrW_2O_8$–$0.30SiO_2$ and (**b**) $0.85ZrW_2O_8$–$0.15SiO_2$; EDS spectra of (**c**) SiO_2 and (**d**) ZrW_2O_8

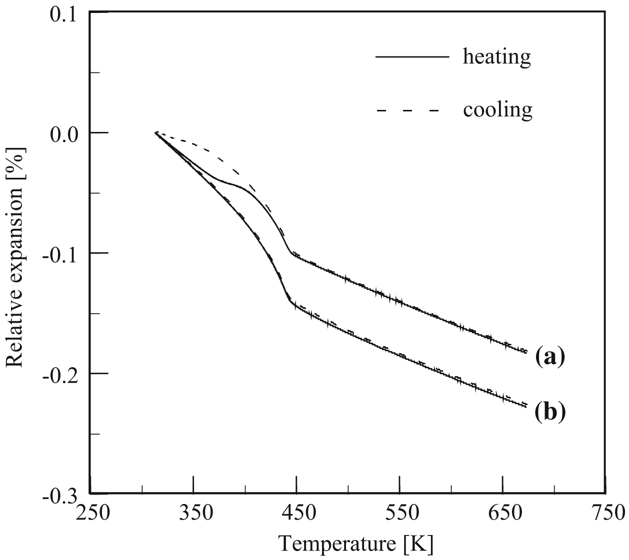

Fig. 4 TMA curves of (a) $0.70ZrW_2O_8$–$0.30SiO_2$ and (b) $0.85ZrW_2O_8$–$0.15SiO_2$

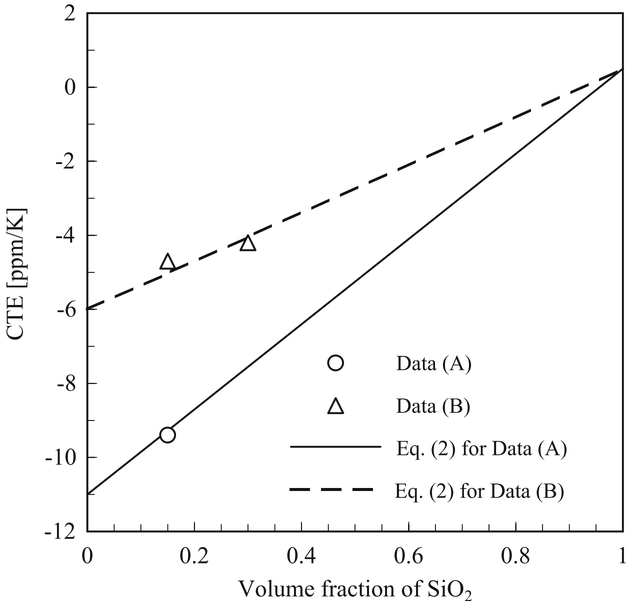

Fig. 5 CTE of ZrW_2O_8–SiO_2 and its fitting to Eq. 2

frequency. The observed ε_r and tanδ behaviors can be rationalized as follows [30]. Dielectric loss in ionic solids results from three primary effects: (1) ion migration losses (dc conductivity), (2) ion vibration and deformation losses, and (3) electron polarization losses. Of these, the most important process is ionic migration loss, which tends to show a large increase in the loss at low frequencies. Therefore, a high value of tanδ of ZrW_2O_8–SiO_2 is probably due to oxygen vacancy.

Table 1 shows the microwave properties of re-oxidized ZrW_2O_8–SiO_2, where Q and f represent the quality factor and the resonant frequency of re-oxidized ZrW_2O_8–SiO_2, respectively. The ε_r of $0.70ZrW_2O_8$–$0.30SiO_2$ was lower than that of $0.85ZrW_2O_8$–$0.15SiO_2$, and thus the

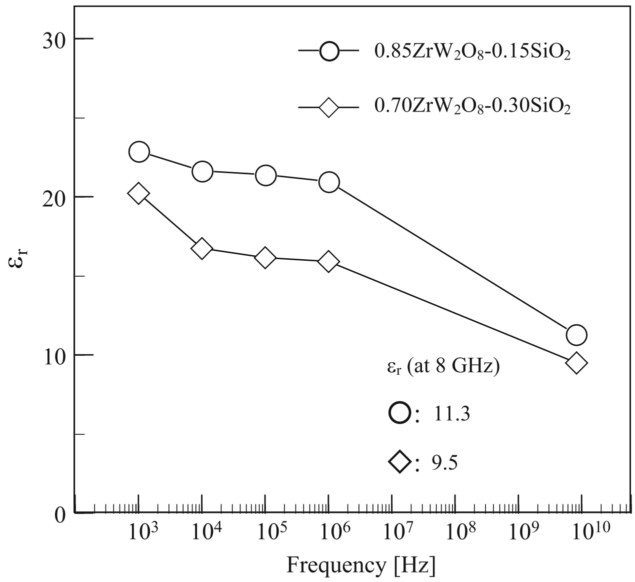

Fig. 6 Frequency dependence of the ε_r of re-oxidized ZrW_2O_8–SiO_2

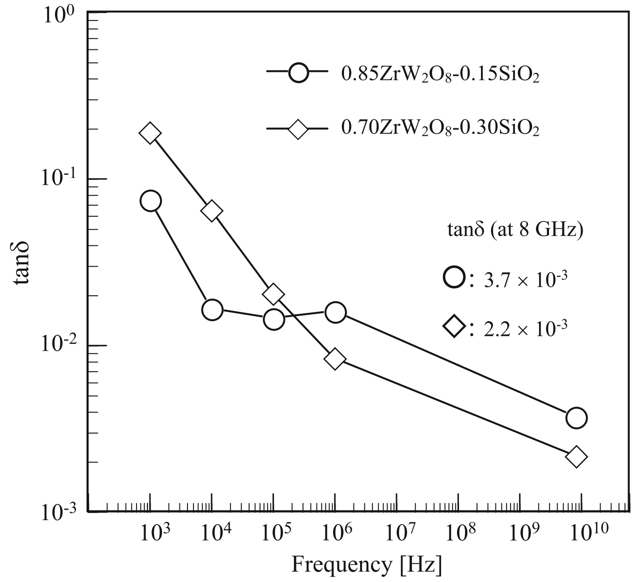

Fig. 7 Frequency dependence of the tanδ of re-oxidized ZrW_2O_8–SiO_2

Table 1 Microwave properties of re-oxidized ZrW_2O_8–SiO_2

Sample	ε_r	*Qf* [GHz]
$0.85ZrW_2O_8$–$0.15SiO_2$	11.3	2200
$0.70ZrW_2O_8$–$0.30SiO_2$	9.5	3800

amorphous SiO_2 phase should be capable of reducing the ε_r of ZrW_2O_8. On the other hand, the *Qf* of $0.70ZrW_2O_8$–$0.30SiO_2$ was higher than that of $0.85ZrW_2O_8$–$0.15SiO_2$, and thus the amorphous SiO_2 phase should be capable of increasing the *Qf* of ZrW_2O_8.

Conclusions

Amorphous ZrW_2O_8 powder and amorphous SiO_2 powder were prepared by a sol–gel process as raw materials, and high-density ZrW_2O_8–SiO_2 were successfully prepared at a much lower temperature of 923 K for a much shorter holding time of 10 min by SPS rather than by conventional melt-quenching method. The relative densities of $0.85ZrW_2O_8$–$0.15SiO_2$ and $0.70ZrW_2O_8$–$0.30SiO_2$ were 99.4% and 96.6%, respectively. The combined technique of a sol–gel process and SPS should enable us to prepare the varied types of high-density composites of ZrW_2O_8 without severe thermal cracking caused by melt-quenching.

The values of both CTE of $0.85ZrW_2O_8$–$0.15SiO_2$ and $0.70ZrW_2O_8$–$0.30SiO_2$ in our study well agreed with the ROM approximation (Eq. 2).

The amorphous SiO_2 phase should be capable of reducing the ε_r of ZrW_2O_8, and also it should be capable of increasing the *Qf* of ZrW_2O_8.

Acknowledgement The authors gratefully thank Mr. M. Hashimoto, Yamaguchi Prefectural Industrial Technology Institute, for helpful suggestions and numerous discussions.

References

1. Sleight AW (1995) Endeavour 19:64
2. Mary TA, Evans JSO, Vogt T et al (1996) Science 272:90
3. Sleight AW (1998) Inorg Chem 37:2854
4. Evans JSO, Mary TA, Sleight AW (1998) Physica B 241–243:311
5. Chang LLY, Scroger MG, Phillips B (1967) J Am Ceram Soc 50:211
6. Graham J, Wadsley AD, Weymouth JH et al (1959) J Am Ceram Soc 42:570
7. Martinek C, Hummel FA (1968) J Am Ceram Soc 51:227
8. Morito Y, Wang S, Ohshima Y et al (2002) J Ceram Soc Jpn 110:544
9. Xing X, Xing Q, Yu R et al (2006) Physica B 371:81
10. Xing Q, Xing X, Yu R et al (2005) J Cryst Growth 283:208
11. Kameswari U, Sleight AW, Evans JSO (2000) Int J Inorg Mater 2:333
12. Closmann C, Sleight AW, Haygarth JC (1998) J Solid State Chem 139:424
13. Wilkinson AP, Lind C, Pattanaik S (1999) Chem Mater 11:101
14. Anselmi-Tamburini U, Gennari S, Garay JE et al (2005) Mater Sci Eng A 394:139
15. Nygren M, Shen Z (2003) Solid State Sci 5:125
16. Shen Z, Johnsson M, Zhao Z et al (2002) J Am Ceram Soc 85:1921
17. Chaim R, Shen ZJ, Nygren M (2004) J Mater Res 19:2527
18. Cha SI, Hong SH, Kim BK (2003) Mater Sci Eng A 351:31
19. Omori M (2000) Mater Sci Eng A 287:183
20. Gupta TK, Jean JH (1996) J Mater Res 11:243
21. Niwa E, Wakamiko S, Ichikawa T et al (2004) J Ceram Soc Jpn 112:271
22. Lommens P, Meyer CD, Bruneel E et al (2005) J Eur Ceram Soc 25:3605
23. Yang X, Xu J, Li H et al (2007) J Am Ceram Soc 90:1953

24. Buysser KD, Lommens P, Meyer CD et al (2004) Ceram-Silik 48:139
25. Yang X, Cheng X, Yan X et al (2007) Compos Sci Technol 67:1167
26. Yilmaz S (2002) J Phys 14:365
27. Yilmaz S, Dunand DC (2004) Compos Sci Technol 64:1895
28. Tani J, Kimura H, Hirota K et al (2007) J Appl Polym Sci 106:3343
29. Kanamori K, Kineri T, Fukuda R et al (2008) J Am Ceram Soc. doi:10.1111/j.1551-2916.2008.02726.x
30. Evans JSO, Mary TA, Vogt T et al (1996) Chem Mater 8:2809
31. Bertoluzza A, Fagnano C, Morelli MA (1982) J Non-Cryst Solids 48:117
32. Nishio K, Kawahara T, Fukuda R et al (2007) J Soc Inorg Mater Jpn 14:69
33. Hashimoto T, Katsube T, Morito Y (2000) Solid State Commun 116:129
34. Hasselman DPH, Donaldson KY, Anderson EM et al (1993) J Am Ceram Soc 76:2180
35. Lind C, Wilkinson AP (2002) J Sol–Gel Sci Technol 25:51